

## Arbitrary Control of a Quantum Electromagnetic Field

C. K. Law and J. H. Eberly

*Rochester Theory Center for Optical Science and Engineering and Department of Physics and Astronomy,  
University of Rochester, Rochester, New York 14627*

(Received 5 October 1995)

We present a cavity QED interaction which forces the ground state of a cavity field mode to evolve into an *arbitrary* quantum state at a prechosen time  $t^*$ . This method does not involve either atom-field state entanglement or the projections characteristic of quantum measurement.

PACS numbers: 42.50.Dv, 03.65.Bz, 42.50.Lc

Controlling the time evolution of quantum systems is an interesting subject that can lead to many useful applications. Generally, we may vary certain time-dependent parameters of a system in order to maximize the overlap between a final state and a desirable quantum state (target state). A fundamental restriction comes from the fact that final states to which an initial state can have access are limited by the Hamiltonian of the system. Therefore an important question is whether we can design a realistic interaction Hamiltonian in order to attain an arbitrary target state at a specific (target) time  $t^*$ .

The question of creating arbitrary quantum states of a cavity field has been discussed in the literature [1–3]. There are two types of difficulties. First, the quantum states of the sources of radiation (i.e., atomic states) have to be manipulated in an arbitrarily controllable manner. Second, we have to design a mechanism so that the source can “teach” the field to evolve toward a desirable quantum state. These difficulties have been approached from different points of view. The methods proposed by Vogel, Akulin, and Schleich [1] and Garraway *et al.* [2] adopt a micromaser-type system in which a two-level atomic beam is used as a radiation source. They assign each atom in the atomic beam a specific state before entering the cavity. After interacting with the field, the quantum states of the atoms are measured. The quantum projection associated with this measurement ensures that the purity of the field state can be maintained. Recently, a scheme has been suggested by Parkins *et al.* [3] which can avoid the uncontrollable (statistical) outcomes of performing these successive quantum measurements. In their method, coherence of Zeeman levels can be mapped onto a cavity field directly via an adiabatic passage mechanism. A basic requirement is that the Zeeman levels have to be initially prepared in prescribed superposition states. Therefore, different target field states need different superpositions of Zeeman levels, and the number of Zeeman levels that is available limits the photon number achievable in the target state.

In this paper, we present a new approach to control quantum states of a cavity field. The major difference between our approach and previous work is that quantum states of the atom (source) are manipulated *during* the

atom-field interaction process, i.e., inside the cavity. Therefore we can create *all target states from the same initial state*. The highest Fock state is not limited by the number of atomic levels, but is limited by values of coupling strengths. Furthermore, we know in advance the specific time  $t^*$  at which the target state is created. Like the method developed by Parkins *et al.* [3], our model does not involve projections characteristic of quantum measurement, and a single atom is sufficient to serve for our purpose. The atom in our approach consists of two effective levels as in the scheme of Vogel, Akulin, and Schleich [1], but we find a significant advantage in a two-channel approach.

We consider a system which consists of a quantized cavity field interacting with a driven quantum system, which we will refer to as an atom, but could also be a trapped ion, for example. We shall show how atom-field interactions can force the vacuum state of the field to evolve into any prespecified superposition of Fock states of finite photon numbers. In other words, general quantum states of the field can be created,

$$|\psi_{\text{target}}\rangle = \sum_{n=0}^M c_n |n\rangle. \quad (1)$$

Here the  $c_n$  are arbitrary complex amplitudes and  $M$  is a prechosen integer which determines the highest Fock state in (1).

The Hamiltonian of our model is given by

$$H(t) = \omega_c a^\dagger a + \frac{1}{2} \omega_0 \sigma_z + [r(t)e^{-i\omega_L t} + g(t)a]\sigma_+ + [r^*(t)e^{i\omega_L t} + g^*(t)a^\dagger]\sigma_-, \quad (2)$$

where  $a^\dagger$  and  $a$  are creation and annihilation operators of a cavity field of frequency  $\omega_c$ . The  $\sigma$ 's describe a two-level atom in the usual Pauli matrix notation. As indicated in Fig. 1, the atom can make transitions between the two levels through two channels. One channel corresponds to the interaction between the atom and an external driving field of frequency  $\omega_L$  and adjustable amplitude. The coupling strength of this channel is characterized by a complex function  $r(t)$ . The second channel is the interaction between the atom and the quantized cavity field, and the corresponding coupling is determined by a complex function  $g(t)$ . Unlike previous studies of the

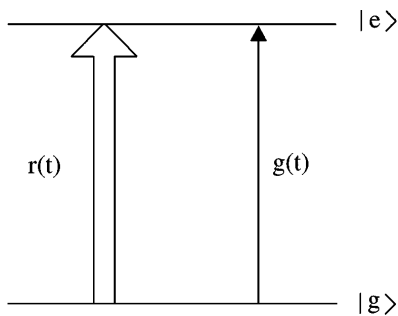


FIG. 1. Schematic drawing of a two-level atom interacting with a cavity mode and a classical driving field.

driven Jaynes-Cummings model [4], we assume that both  $r(t)$  and  $g(t)$  are prescribed functions of time. A possible realization of such a model will be discussed later in this paper.

Under the resonance condition  $\omega_c = \omega_L = \omega_0$ , the Hamiltonian can be written (in the interaction picture) as

$$H_I(t) = [r(t) + g(t)a]\sigma_+ + [r^*(t) + g^*(t)a^\dagger]\sigma_- . \quad (3)$$

We choose the simplest state,

$$|\Psi(0)\rangle = |0, g\rangle, \quad (4)$$

as our initial state, i.e., the cavity field is in the vacuum state and the atom is in the ground state. Our goal is to force the system to evolve into a final state of the form

$$|\Psi(t^*)\rangle = \sum_{n=0}^M c_n |n, g\rangle, \quad (5)$$

after a target time  $t^*$ . Note that the state of the field is the same as the target state  $|\psi_{\text{target}}\rangle$  given in Eq. (1). Since Eq. (5) indicates that *the atom and the field do not entangle*, the state of the field remains pure. (We shall ignore relaxation effects coming from spontaneous atomic decay and cavity damping. This can be justified if  $t^*$  is significantly shorter than both relaxation times.)

Now we describe the strategy of our model. We first divide the time interval  $[0, t^*]$  into  $2M$  subintervals. For simplicity, we let all subintervals have equal lengths, i.e.,  $0 < \tau < 2\tau \dots < j\tau < (j+1)\tau \dots < (2M-1)\tau < t^*$  where  $\tau = t^*/2M$  is defined. Next we assign the following rules such that only one channel is effective at a time: For  $2(j-1)\tau < t < (2j-1)\tau$ ,

$$r(t) = r_j, \quad g(t) = 0. \quad (6)$$

For  $(2j-1)\tau < t < 2j\tau$ ,

$$r(t) = 0, \quad g(t) = g_j, \quad (7)$$

where  $r_j$  and  $g_j$  ( $1 \leq j \leq M$ ) are complex constants to be determined.

The time evolution operator of the system can be expressed as a product of a sequence of evolution operators associated with the time intervals, i.e.,

$$U(t^*) = Q_M C_M Q_{M-1} C_{M-1} \dots Q_2 C_2 Q_1 C_1. \quad (8)$$

Here  $Q_j$  describes the evolution due to the quantized field channel and  $C_j$  describes the evolution due to the

classical field channel. Both  $Q_j$  and  $C_j$  can be expressed analytically in the form of a  $2 \times 2$  matrix with respect to the atomic basis,

$$Q_j = \begin{pmatrix} \cos |g_j| \sqrt{aa^\dagger} \tau & -ia e^{i\phi_j} \frac{\sin |g_j| \sqrt{a^\dagger a} \tau}{\sqrt{a^\dagger a}} \\ -ia^\dagger e^{-i\phi_j} \frac{\sin |g_j| \sqrt{aa^\dagger} \tau}{\sqrt{aa^\dagger}} & \cos |g_j| \sqrt{a^\dagger a} \tau \end{pmatrix}, \quad (9)$$

$$C_j = \begin{pmatrix} \cos |r_j| \tau & -ie^{i\theta_j} \sin |r_j| \tau \\ -ie^{-i\theta_j} \sin |r_j| \tau & \cos |r_j| \tau \end{pmatrix}. \quad (10)$$

Here we have let  $r_j = |r_j| e^{i\theta_j}$ , and  $g_j = |g_j| e^{i\phi_j}$ .

The final step is to determine the values of  $\{r_j\}$  and  $\{g_j\}$ . This can be done by solving the equation of inverse evolution,

$$|0, g\rangle = U(-t^*) |\Psi(t^*)\rangle \\ = C_1^\dagger Q_1^\dagger C_2^\dagger Q_2^\dagger \dots C_M^\dagger Q_M^\dagger |\Psi(t^*)\rangle. \quad (11)$$

For an arbitrary  $|\Psi(t^*)\rangle$  given in the form of Eq. (5), we can always find a solution for  $\{r_j\}$  and  $\{g_j\}$ . This can be done because the sequence of operators in the right side of Eq. (11) can remove photons successively from the state  $|\Psi(t^*)\rangle$  until all the photons are exhausted. More specifically, the values for  $\{r_j\}$  and  $\{g_j\}$  can be determined by solving the following equations,

$$\alpha_j \cos |g_j| \sqrt{j} \tau + i\beta_j e^{-i\phi_j} \sin |g_j| \sqrt{j} \tau = 0, \quad (12)$$

$$\mu_j \cos |r_j| \tau + i\nu_j e^{i\theta_j} \sin |r_j| \tau = 0. \quad (13)$$

The coefficients  $\alpha_j$ ,  $\beta_j$ ,  $\mu_j$ , and  $\nu_j$  ( $1 \leq j \leq M$ ) are given by

$$\alpha_j = \langle j, g | F_{j+1} \rangle, \quad (14)$$

$$\beta_j = \langle j-1, e | F_{j+1} \rangle, \quad (15)$$

$$\mu_j = \langle j-1, e | Q_j^\dagger | F_{j+1} \rangle, \quad (16)$$

$$\nu_j = \langle j-1, g | Q_j^\dagger | F_{j+1} \rangle, \quad (17)$$

with

$$|F_j\rangle \equiv C_j^\dagger Q_j^\dagger C_{j+1}^\dagger Q_{j+1}^\dagger \dots C_M^\dagger Q_M^\dagger |\Psi(t^*)\rangle \quad (18)$$

and  $|F_{M+1}\rangle \equiv |\Psi(t^*)\rangle$ . Equations (12) and (13) ensure that when  $C_j^\dagger Q_j^\dagger$  acts on  $|F_{j+1}\rangle$ , all populations in  $|j, g\rangle$  and  $|j-1, e\rangle$  are transferred to  $|j-1, g\rangle$ . Therefore by repeating the process,  $|\Psi(t^*)\rangle$  can be brought into  $|0, g\rangle$  as required in Eq. (11).

Since a solution for (12) and (13) always exists (in fact more than one), we have established the fact that arbitrary target states can be obtained at the time  $t^*$ . It should be noted that the prechosen value of  $M$  for the highest Fock state number can be arbitrarily large, but is restricted in practice because  $r(t)$  and  $g(t)$  are finite in real physical systems. However, if we do not restrict the  $2M$  time intervals to have equal lengths, we may treat the durations of the time intervals as adjustable parameters. In doing so, the model becomes more flexible and it is

possible to optimize the number  $M$  for a given target time  $t^*$ . Suppose that the largest possible coupling strengths are given by  $g_{\max}$  and  $r_{\max}$ . It can be shown that the condition

$$t^* > \frac{M\pi}{2r_{\max}} + \frac{\pi}{2g_{\max}} \sum_{j=1}^M \frac{1}{\sqrt{j}} \quad (19)$$

determines the biggest  $M$  that our model can reach [5]. For example, we can have  $M \leq 10$  for a moderately strong coupling  $g_{\max}t^* = 25$  and  $r_{\max} = g_{\max}$ .

As an illustration, we show in Table I the values of  $\{r_j\}$  and  $\{g_j\}$  in order to create the state,

$$|\psi_{\text{target}}\rangle = \frac{1}{\sqrt{3}}\{|0\rangle + |5\rangle + |10\rangle\}. \quad (20)$$

This state is a superposition of three distinct Fock states, and although Eq. (20) looks so simple, the corresponding phase-space distribution  $Q(\alpha) = |\langle\alpha|\psi_{\text{target}}\rangle|^2$  (where  $|\alpha\rangle$  are coherent states) is rather remarkable. As we can see from the contour plot of  $Q(\alpha)$  in Fig. 2, the interference between the three Fock states yields flowerlike contours. We may perhaps call this state a “flower” state. It is worth noting that the creation of  $|\psi_{\text{target}}\rangle$  is not sensitive to small errors in  $\{r_j\}$  and  $\{g_j\}$ . We have tested the stability using only two significant figures in each  $r_j$  and  $g_j$  in Table I, and found that the final state still has 96% overlap with the target state.

Finally we discuss a possible realization of our model in a cavity QED configuration. The driven Jaynes-Cummings model cannot be applied here because the coupling strength  $g(t)$  must be variable in an arbitrarily prescribed way. However, this problem can be overcome just by using a two-channel Raman interaction [6,7], as shown in Fig. 3. In this case, a three-level atom can be excited via two Raman channels. One channel contains two classical external fields  $\vec{E}_p(t)$  and  $\vec{E}_s(t)$ , and they have frequencies  $\omega_p$  and  $\omega_s$ , respectively. We assume that the frequencies satisfy the usual Raman resonance condition  $\omega_p - \omega_s = \omega_0$ , where  $\omega_0$  is the energy difference between levels  $|3\rangle$  and  $|1\rangle$ . The second channel contains a classical external field  $\vec{E}_g(t)$  with a frequency

$\omega_g$ , and the quantized cavity field of frequency  $\omega_c$ . The electric field operator of the cavity mode can be expressed as  $\vec{E}_c = \kappa(a + a^\dagger)\vec{e}_\lambda$ , where  $\vec{e}_\lambda$  is the polarization vector and  $\kappa$  is determined by the quantization volume. As in the first channel, we assume the Raman resonance condition  $\omega_g - \omega_c = \omega_0$  to be satisfied. Notice that  $\vec{E}_p(t)$ ,  $\vec{E}_s(t)$ , and  $\vec{E}_g(t)$  are envelopes of driving fields which can be varied externally. If the detunings  $\Delta_a$  and  $\Delta_b$  are sufficiently large, the upper level can be adiabatically eliminated [6]. It can be shown that the effective Hamiltonian has the same form as Eq. (3), in which we can identify the two levels  $|1\rangle, |3\rangle$  as  $|g\rangle, |e\rangle$  and the couplings

$$r(t) = -\frac{[\vec{d}_{21} \cdot \vec{E}_p(t)][\vec{d}_{32} \cdot \vec{E}_s^*(t)]}{\Delta_a}, \quad (21)$$

$$g(t) = -\frac{[\vec{d}_{21} \cdot \vec{E}_g(t)](\vec{d}_{32} \cdot \kappa\vec{e}_\lambda)}{\Delta_b}. \quad (22)$$

Here  $\langle i|\vec{d}|k\rangle$  ( $i, k = 1, 2, 3$ ) are atomic dipole matrix elements. Therefore by switching on and off the classical fields with correct amplitudes and phases, the required time dependence of  $r(t)$  and  $g(t)$  can be obtained. We remark that there should be terms describing small ac Stark shifts in the effective Hamiltonian, which we ignore here.

To conclude, we have presented a cavity QED model which allows the vacuum state to evolve to an *arbitrarily prescribed superposition* of Fock states. Our model basically transforms the problem of controlling a quantized field into the problem of controlling the time sequences of amplitudes and phases of  $r(t)$  and  $g(t)$ . This also includes a precise knowledge of the starting time  $t = 0$ , so that the system can be initiated correctly. These technical difficulties are perhaps the only price for arbitrary control of a quantum field. From a theoretical point of view, the

TABLE I. Numerical solutions of  $\{r_j\}$  and  $\{g_j\}$  for creating the target state in Fig. 2.

$j$	$g_j\tau$	$r_j\tau$
1	1.5560	1.2874
2	0.7283	-1.1748
3	-0.8322	-1.3744
4	0.7594	1.4900
5	0.6553	1.2629
6	-0.6211	-1.2475
7	-0.5879	-1.2549
8	0.5554	-1.1702
9	0.5236	1.5708
10	0.4967	1.5708

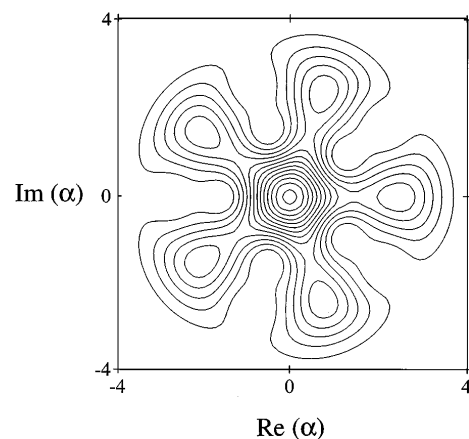


FIG. 2. Contour plot of the  $Q$  function for the target state:  $|\psi_{\text{target}}\rangle = 3^{-1/2}\{|0\rangle + |5\rangle + |10\rangle\}$ . Contour lines are taken at  $Q(\alpha) = 0.027n$ , where  $n = 1, 2, \dots, 15$ . The highest contour corresponds to the small circle around the origin. The outermost contour has the lowest height.

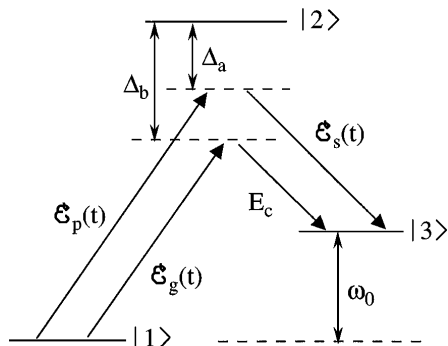


FIG. 3. A two-channel Raman transition diagram. The envelopes of driving fields are labeled by  $\vec{E}_p(t)$ ,  $\vec{E}_s(t)$ , and  $\vec{E}_g(t)$ . In order to make the two channels distinct from each other, the energy difference  $\omega_0$  has to be significantly larger than the bandwidths of the fields, as well as the Rabi frequencies associated with each channel.

fact that our model can access all possible quantum states is interesting and may suggest useful applications. We hope to address questions about the influence of noise in  $r(t)$  and  $g(t)$ , as well as the turn-on effects of the fields in the future.

This research was partially supported by NSF Grants No. PHY 94-08733 and No. PHY94-15583.

- [1] K. Vogel, V.M. Akulin, and W.P. Schleich, Phys. Rev. Lett. **71**, 1816 (1993).

- [2] B.M. Garraway, B. Sherman, H. Moya-Cessa, and P.L. Knight, Phys. Rev. A **49**, 535 (1994).
- [3] A.S. Parkins, P. Marte, P. Zoller, and H.J. Kimble, Phys. Rev. Lett. **71**, 3095 (1993); A.S. Parkins, P. Marte, P. Zoller, O. Carnal, and H.J. Kimble, Phys. Rev. A **51**, 1578 (1995).
- [4] P. Alsing, D.S. Guo, and H.J. Carmichael, Phys. Rev. A **45**, 5135 (1992); I.V. Jyotsna and G.S. Agarwal, Opt. Commun. **99**, 334 (1993); S.M. Dutra, P.L. Knight, and H. Moya-Cessa, Phys. Rev. A **49**, 1993 (1994).
- [5] To derive condition (19), we divide the time interval  $[0, t^*]$  into  $2M$  subintervals of *unequal* lengths, i.e.,  $0 = t_0 < t_1 < t_2 \cdots < t_k < t_{k+1} \cdots < t_{2M-1} < t_{2M} = t^*$ . When maximum couplings  $r_{\max}$  and  $g_{\max}$  are given, the biggest  $M$  allowed to create arbitrary states (1) is determined by (19). This corresponds to the time sequence  $t_{2j} - t_{2j-1} = \pi/2g_{\max}\sqrt{j}$  and  $t_{2j-1} - t_{2j-2} = \pi/2r_{\max}$ .
- [6] Liwei Wang, R.R. Puri, and J.H. Eberly, Phys. Rev. A **46**, 7192 (1992); C.K. Law and J.H. Eberly, Phys. Rev. A **47**, 3195 (1993); Liwei Wang and J.H. Eberly, Phys. Rev. A **47**, 4248 (1993).
- [7] Two-channel Raman processes are also found useful in preparing nonclassical states of motion of a trapped ion; see J.I. Cirac, A.S. Parkins, R. Blatt, and P. Zoller, Phys. Rev. Lett. **70**, 556 (1993); C. Monroe, D.M. Meekhof, B.E. King, S.R. Jefferts, W.M. Itano, D.J. Wineland, and P. Gould, Phys. Rev. Lett. **75**, 4011 (1995); D.M. Meekhof *et al.* (private communication).